Vibrational dynamics as an indicator of short-time interactions in glass-forming liquids and their possible relation to cooperativity

ARTICLE *in* THE JOURNAL OF CHEMICAL PHYSICS · JULY 2002

Impact Factor: 2.95 · DOI: 10.1063/1.1484103

2 AUTHORS:

Sviatoslav Kirillov
Joint Department of Electrochemical Energy …
91 PUBLICATIONS **531** CITATIONS

SEE PROFILE

Spyros N. Yannopoulos
Foundation for Research and Technology - H…
139 PUBLICATIONS **1,818** CITATIONS

SEE PROFILE

Vibrational dynamics as an indicator of short-time interactions in glass-forming liquids and their possible relation to cooperativity

Sviatoslav A. Kirillov[a)]
Institute for Technological and Information Innovations, P.O. Box 263, 03134 Kyiv-134, Ukraine, and Institute for Sorption and Problems of Endoecology, Ukrainian National Academy of Sciences, Gen. Naumov St. 13, 03142 Kyiv-142, Ukraine

Spyros N. Yannopoulos[b)]
Foundation for Research and Technology—Hellas, Institute of Chemical Engineering and High-Temperature Chemical Processes (FORTH-ICE/HT), P.O. Box 1414, 265 00 Patras, Greece

(Received 24 January 2002; accepted 17 April 2002)

We report on a vibrational dynamics study of two glass-forming liquids over a wide temperature range including the glassy, supercooled, and molten state. Our aim is to find possible sensitive indicators of short-time dynamics that experience characteristic changes when approaching the liquid–glass transition. The observed changes in vibrational dynamics are employed to track the cooperative behavior of the studied glass-forming liquids. It has been found that both strong and fragile liquids exhibit qualitative similarities in the vibrational relaxation and frequency modulation times as a function of temperature. The temperature dependence of the vibrational relaxation times τ_V experiences a break at the glass transition temperature T_g. On the contrary, the temperature dependence of the frequency modulation times τ_ω exhibits an unexpected discontinuity at T_g, τ_ω being shorter in the glassy phase than in the supercooled and liquid regime. Since microscopic vibrational dynamics depends upon the intermolecular interactions that ultimately are responsible for the cooperative (or sluggish) dynamics when approaching T_g, an attempt has been made to find a rationale between the unusual temperature dependence of τ_ω and cooperative dynamics. © *2002 American Institute of Physics.* [DOI: 10.1063/1.1484103]

I. INTRODUCTION

One of the important goals in contemporary condensed matter physics is a comprehensive achievement of a microscopic description for the different aspects of the dynamic glass transition.[1] It has been recognized that the major difficulty to comprehend the glass transition-related issues lies in the complications imposed by the mutual interactions between molecular units,[2] an issue known also as the *many-body* problem.

In the framework of the coupling model[2] for relaxation there is a gradual transition from single-molecule dynamics to many-particle dynamics where intermolecular interactions come into play. The latter are manifested through the fractional (or stretching) exponent of the nonexponential relaxations for any autocorrelation function relevant to the glass transition dynamics. The main structural or α-relaxation process in supercooled liquids succeeds much faster microscopic motions, such as fast relaxations characterized by picosecond dynamics and vibrational degrees of freedom acting in the subpicosecond time domain. Further, the temperature-dependent activation energy of the viscosity or the structural α-relaxation time of the supercooled liquid approaching the glass transition temperature, T_g, has also been considered as an indication of many-body interactions, or as the cooperativity onset.[3]

From a different point of view, it is so far a well-established concept to those working on vibrational dephasing mechanisms in liquids that vibrational energy levels and therefore vibrational frequencies experience the influence of their immediate environment when going from the gas (isolated) phase to the liquid (condensed) phase.[4] In this case, the mechanisms of energy flow into and out of a molecule and other related points are the important issues to be addressed.

The present work aims at finding a possible connection between the two aforementioned aspects. In particular, we will try to tackle the question of whether or not microscopic dynamics emerging from vibrational dephasing studies can be used as a sensitive indicator of the cooperativity, as this is evidenced in the viscosity (or α-relaxation time) deviation from the expected Arrhenius behavior in supercooled liquids. To accomplish our task we have employed a temperature-dependence Raman spectroscopic study for two inorganic glass-formers of different fragility. The strong liquid As_2O_3 and the fragile $2BiCl_3$–KCl have been studied experimentally in their glassy, supercooled, and molten states. Intramolecular vibrational modes have been analyzed by means of a specific algorithm that allows us to extract time-correlation functions without Fourier transforming the experimental data. We thus avoid all the concomitant inaccuracies that such Fourier transform (FT) techniques convey when applied to noisy and overlappping vibrational lines.

The paper is organized as follows: In Sec. II we present a short background on cooperativity, vibrational relaxation, and time-correlation functions needed for analyzing Raman

a)Electronic mail: kir@i.kiev.ua
b)Electronic mail: sny@iceht.forth.gr

spectra. Section III contains the experimental details, i.e., chemical preparation and light scattering apparatus. Section IV is devoted to the presentation and discussion of the results obtained. Finally, the main conclusions that can be drawn from this study are summarized in Sec. V.

II. BACKGROUND

A. Some remarks on cooperativity

When particular liquids are supercooled sufficiently below the melting temperatures T_m of their corresponding crystals, structural rearrangements and translational displacements of the molecules occur very slowly and demand correlated motion over their ''local environment.'' This kind of motion has been called cooperative and the linear dimension of the volume of the environment mentioned defines the cooperative length of the glass transition.[3,5] Based on the definition of the cooperative length, it is obvious that this quantity depends on specific characteristics of the material such as chemical bonding, geometrical characteristics of the relaxing unit, spatial extent of the medium range order, dimensionality of the space that accommodates the relaxators, etc. The cooperativity length is a genuine *dynamic feature* of supercooled liquids, and as such cannot be revealed through standard diffraction experiments. It can instead be inferred indirectly from measurements of dynamic or thermodynamic properties.[5]

Originally, the concept of cooperativity was introduced by Adam and Gibbs in an attempt to combine relaxation with configurational entropy.[3] In their phenomenological model, they proposed a link between the relaxation time and the size of a cooperative domain. The latter is identified as the smallest group of molecules needed to perform a correlated motion in a relaxation step, e.g., $\tau^{-1} \propto \exp(-\alpha V_c)$, where α is a constant and V_c the cooperative volume supposed to be inversely proportional to the configurational entropy. The number of ''cooperative units,'' which constitute the cooperative volume, has been determined from thermodynamic data and exhibits a temperature behavior that bears a close resemblance to the temperature dependence of other dynamic parameters such as the fragility and the stretching exponent of the correlation function describing structural relaxation.[6]

Signatures of cooperativity can be found in numerous model descriptions of glassy dynamics. For instance, the coupling model for relaxation[2] intrinsically includes cooperativity in the stretching exponent of the relevant autocorrelation function related to glass dynamics. Simulation approaches dealing with lattice gas[7(a)] and Ising spin[7(b)] models under certain conditions are shown to exhibit cooperative dynamics. In molecular dynamics studies[8(a)] a characteristic cooperative length has been identified with the largest wavelength-propagating transverse mode that a liquid can support, and the nature of cooperative motions has been ascribed to stringlike molecular movements.[8(b)]

On the experimental side, numerous approaches have been used to estimate the cooperativity length,[9] though having the disadvantage of perturbing the system studied by changing side groups in glass-forming polymers or adding trace molecules. In all cases so far, the correlation length has been found to spread over the range 2–5 nm. A more direct observation has been achieved recently by means of nanometer-scale probing of dielectric fluctuations and analysis of random noise.[10] In particular, it has been revealed that molecular cooperativity near T_g in poly (vinyl acetate) takes the form of transient reorienting molecular clusters of a few nanometers in size.

B. Vibrational relaxation and dephasing in liquids

1. General remarks

It becomes obvious from Sec. II A that the individual dynamics of molecules bound in ''cooperative regions'' should also experience changes as the temperature of a supercooled liquid is decreased and the cooperative motions become imperative. Particular properties of a molecule's vibrational response such as energy relaxation, dephasing, etc. are considered to be rather sensitive indicators of the intermolecular interactions. The latter are essentially the decisive factors of cooperative behavior.

In general, vibrational relaxation arises from the picosecond interaction (coupling) of the probe particle and its surroundings. Diagonal terms in the coupling Hamiltonian characterize pure dephasing, i.e., the process in which the amplitudes of different states become uncorrelated. Nondiagonal terms in the coupling Hamiltonian describe the population (energy) relaxation. A detailed treatment of these phenomena can be found in the series of reviews by Oxtoby[11] (for more recent surveys see Ref. 12). Fast dephasing processes contribute to the *homogeneous* part of the vibrational line profile, while slow dephasing leads to the *inhomogeneous* component; these terms will become more clear in the next section. It is customary to consider that energy relaxation processes are relatively slow and that they contribute to the inhomogeneous part of line shape. Finally, it would be helpful to recall that the width of the vibrational line profile relates to the inverse of the respective characteristic relaxation time.

First attempts to tackle the issue of short-time dynamics in glass-forming systems by means of vibrational spectroscopy have sought possible dynamical indicators distinguishing between the supercooled liquid and glassy state for molten nitrates.[13(a)] It was found that the temperature dependence of Raman linewidths in KNO_3–$Ca(NO_3)_2$ and $RbNO_3$–$Ca(NO_3)_2$ systems undergoes a break at temperatures well below T_m. Similar observations made even earlier[13(b)] noticed that the temperature dependence of linewidth of a particular band of As_2O_3 experiences a break at T_g. Later one, breaks in the temperature dependence of Raman linewidths were reported for glass-forming sulphate systems.[13(c)]

All the aforementioned data have been obtained by means of ''ordinary'' vibrational spectroscopy (Raman or IR), which operates in the frequency domain and cannot discriminate between the homogeneous and inhomogeneous contribution to the observed linewidth. This discrimination could be attained by means of more powerful time-domain techniques like vibrational echo studies. Such approaches, recently applied to some glass-forming organic materials,[14]

have led to similar temperature dependencies of characteristic times, i.e., they exhibit a break around T_g.

Based on this brief survey, we see that breaks in the temperature dependence of Raman linewidths might be a common feature of glass-forming systems, and an analysis of vibrational dephasing mechanisms in these systems below and above T_g may help to find signatures of cooperativity. To achieve this goal, time-domain techniques are definitely more suitable. However, it will be shown in the following that even conventional Raman methods supported with proper theoretical analysis can provide useful information concerning vibrational dephasing mechanisms, allowing cooperativity related issues to be addressed.

2. Time-correlation functions for analyzing Raman spectra

One of the remarkable features in spectroscopic studies is that a wealth of molecular dynamics is buried in spectral line shapes.[11,15] In particular, it has been demonstrated that the information obtained in the frequency domain and the information acquired in the time domain are equivalent, and an experimentally measured spectrum $I(\omega)$ can be translated into a time-correlation function (TCF) $G(t)$ by means of a simple Fourier transform, i.e.,

$$I(\omega)=\frac{1}{2\pi}\int_{-\infty}^{+\infty}dt\,\exp(-i\omega t)G(t), \tag{1}$$

where ω is the frequency in s^{-1} and t is the time.

In the Raman spectroscopic study that we undertake in this work, the vibrational relaxation TCF of interest $G_V(t)$ is related through Eq. (1) to the isotropic component of the measured Raman profile defined as

$$I_{\mathrm{iso}}(\omega)=I_{VV}(\omega)-\tfrac{4}{3}I_{HV}(\omega), \tag{2}$$

where $I_{HV}(\omega)$ and $I_{VV}(\omega)$ denote the scattered intensities with the electric field propagating in a direction perpendicular and parallel to that of the incident radiation electric field, respectively.

The description of pure dephasing[15(b),16] remains one of the crucial steps in any theory dealing with vibrational relaxation, since any act of energy transfer inevitably leads to a phase shift. This is based on expressing $G_V(t)$ as

$$G_V(t)=\exp\left(-\int_0^t dt'\int_0^{t'}dt''\langle\Delta\omega(t')\Delta\omega(t'')\rangle\right), \tag{3}$$

where $\Delta\omega(t)$, the instantaneous vibrational frequency of a molecule, is a stochastic variable changing in time due to energy fluctuations (perturbations) caused by translational and rotational motion of the probe particle and its surroundings: $\Delta\omega(t)\propto f(r,t)$, where $f(r,t)$ is the space- and time-dependent potential of molecular interactions. The angular brackets in Eq. (3) refer to an ensemble average over translational and rotational degrees of freedom. Expanding Eq. (3) in terms of cumulant averages, considering $\Delta\omega(t)$ a Gaussian random process with zero mean, and introducing the TCF of frequency modulation $G_\omega(t)$ as

$$G_\omega(t)=\frac{\langle\Delta\omega(t)\Delta\omega(0)\rangle}{\langle\Delta\omega(0)^2\rangle}=\frac{\langle\Delta\omega(t)\Delta\omega(0)\rangle}{M_2}, \tag{4}$$

one gets

$$G_V(t)=\exp\left[-M_2\int_0^t dt(t-t')\right]G_\omega(t), \tag{5}$$

where $M_2=\int_{-\infty}^{+\infty}\omega^2 I_{\mathrm{iso}}(\omega)d\omega$ is the vibrational second moment (perturbation dispersion).

If $G_\omega(t)$ is taken in the simplest, exponential form (Gaussian—Markovian modulation process with short phase memory)

$$G_\omega(t)=\frac{\langle\Delta\omega(t)\Delta\omega(0)\rangle}{M_2}=\exp(-t/\tau_\omega), \tag{6}$$

then Eq. (5) reduces to the well-known Kubo–Rothschild expression

$$G_V(t)=\exp\{-M_2\tau_\omega^2[\exp(-t/\tau_\omega)-1+t/\tau_\omega]\}. \tag{7}$$

The valuable ingredient of this theory is the prediction of a limiting behavior of $G_V(t)$ and respective line profiles, $I_{\mathrm{iso}}(\omega)$. If $\tau_\omega\to\infty$ (the modulation process is slow), or when $t\to 0$, then

$$G_V(t)=\exp(-\tfrac{1}{2}M_2t^2)=\exp(-\tfrac{1}{2}\pi t^2/\tau_V^2), \tag{8}$$

where $\tau_V=\int_0^\infty G_V(t)dt$ is the characteristic time of vibrational dephasing. In this slow modulation limit (''static'' case, frozen environment, inhomogeneous broadening) the time-correlation function is Gaussian and the profile of the corresponding vibrational line is also Gaussian. If the modulation process is fast, $\tau_\omega\to 0$, or when $t\to\infty$

$$G_V(t)=\exp(-M_2\tau_\omega t)=\exp(-t/\tau_V). \tag{9}$$

In this fast modulation limit (homogeneous broadening) the time-correlation function is exponential and the line profile in the frequency domain is Lorentzian. In the intermediate regime, line profiles could be described by the Voigt function, which does not, however, have an analytic Fourier transform.

The mathematical apparatus applied by more specific models of vibrational dephasing (see, e.g., Ref. 17) employs the so-called force-force fluctuation TCF, $\langle\Delta F(t)\Delta F(0)\rangle$. The latter is proportional to the TCF of frequency modulation, $\langle\Delta F(t)\Delta F(0)\rangle\propto\langle\Delta\omega(t)\Delta\omega(0)\rangle$; such an idea goes back to works of Zwanzig.[18] Parenthetically, it should be mentioned that the proportionality between the force–force TCF and the TCF of the frequency modulation serves as a cornerstone for numerous useful applications like modeling vibrational dephasing processes by means of molecular dynamics simulations[19] and calculations of memory functions for vibrational dephasing.[20]

Pure dephasing in ordinary liquids is usually considered a phenomenon involving short-range repulsion potentials,[17] although several models accounting for long-range attraction forces are also known.[17(b)] It should be noticed that dephasing phenomena caused by repulsion forces are often supposed to generate homogeneous line profiles, whereas phenomena caused by attraction result in inhomogeneously broadened lines. From the theoretical point of view, limiting

homogeneous cases are achieved in terms of the time integral over the force–force fluctuation TCF, and therefore retain the dependence on the force–force fluctuation (collision, modulation) time. In inhomogeneous cases, time dependencies are usually ignored by construction: since potentials involved are long-range ones, the dephasing times are determined primarily by static, structural (spatial) averages over solvent–solute force fluctuations and therefore do not feel any short-time ''noise.'' This means that dephasing studies sometimes enable one to roughly distinguish between different types of (spectroscopically discernible) forces prevailing in the system studied.

III. EXPERIMENTS

Ultrapure chemicals are of vital importance for obtaining high-quality data in light scattering spectroscopies. Inorganic substances and especially halide (chloride) materials present a particular difficulty in their handling due to the high sensitivity that they present to moisture.

The purification procedure followed in order to obtain ultrapure arsenic trioxide (purchased from Merck Chemical company) have been described previously.[21(a),21(b)] The optical cells, fused silica tubes with 10 mm o.d.—8 mm i.d., after careful cleaning were loaded with the chemical and were flame sealed under vacuum. The loading procedure involves sublimation of As_2O_3 directly into the optical cells, since a filtration process of the present system is impossible due to the extremely high viscosity of the melt even at temperatures far above the melting point T_m of the corresponding crystal. Before spectra recording the samples were kept at about 400 °C for several hours until the disappearance of the bubbles formed during the melting. Characteristic temperatures for As_2O_3 are $T_g \approx 160$ °C and $T_m \approx 312$ °C.

For the bismuth–potassium chloride mixture, the starting materials $BiCl_3$ (purity ~98%) and KCl (purity ~99%) were both purchased from Merck. They were subsequently purified by successive sublimations under vacuum ($BiCl_3$) and by recrystallization of the melt under inert atmosphere conditions (KCl). The purified materials were then mixed in the appropriate mole composition, 66.6% $BiCl_3$ and 33.4% KCl, in the optical cells. Chlorine gas was subsequently added to the optical cells in order to avoid reduction of Bi at higher temperatures. Such reduction would produce a deep red coloration, which was not observed in our work. More details can be found elsewhere.[21(c)] Characteristic temperatures for $2BiCl_3$–KCl are $T_g \approx 37$ °C and $T_m \approx 167$ °C.

Right-angle Raman spectra were recorded with a 0.85 m double monochromator (Spex 1403). The excitation source was an Ar^+ laser (Spectra Physics) operating at the 514.5 nm line with an output power of about 100 mW. The instrumental resolution was fixed at 1.5 cm^{-1} for the whole set of measurements, and the temperature was controlled with an accuracy of ~1 K. Both scattering geometries, VV and HV, were employed. The signal after its detection from a water-cooled photomultiplier and its amplification from standard electronic equipment was transferred to a computer. Representative Raman spectra for both glasses are shown in Fig. 1.

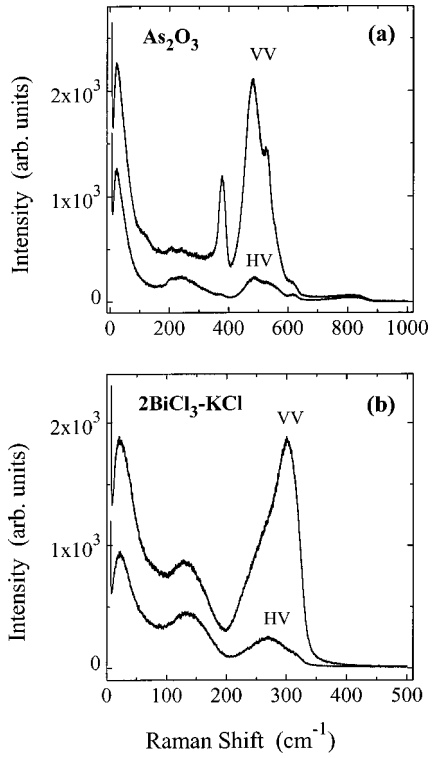

FIG. 1. Representative polarized (VV) and depolarized (HV) spectra for (a) As_2O_3, (b) $2BiCl_3$–KCl at room temperature.

IV. RESULTS AND DISCUSSION

A. Vibrational dephasing and vibrational frequency modulation at temperatures around T_g: Experimental data

The spectra presented in Fig. 1 can be divided into two main regions, the low-frequency (below ~150 cm^{-1}) and the high-frequency (above ~150 cm^{-1}) Raman region. In the former one, the quasielastic scattering (that is, a relaxational contribution centered at zero frequency) and the Boson peak (the vibrational part corresponding to acoustical phonons which become Raman active due to the breakdown of selection rules in glasses, if compared to perfect crystals), show up. In ionic glass-forming systems, an extra contribution to the relaxation part exists, having its origin in scattering caused by charge-current fluctuations. All these issues have been thoroughly discussed in Ref. 21 from both theoretical[21(c)] and experimental [As_2O_3[21(b)] and $2BiCl_3$–KCl[21(c)]] points of view and will not be further mentioned here. In the present paper our main concern is vibrational dynamics; therefore, we will focus our attention on the high-frequency Raman region, and in particular above ca. 250 cm^{-1}, where vibrations of structural entities forming the glass can be studied. However, due to the strong overlap of the two regions the low-frequency spectrum was taken into account in the fitting procedure in order to determine accurately the spectral features of the high-frequency Raman peaks. The analytical models, used in this work for the low-frequency data treatment, have been described elsewhere.[21(c)]

A detailed analysis of the isotropic and anisotropic Raman spectra of the systems studied has been performed together with an examination of the depolarization ratio spec-

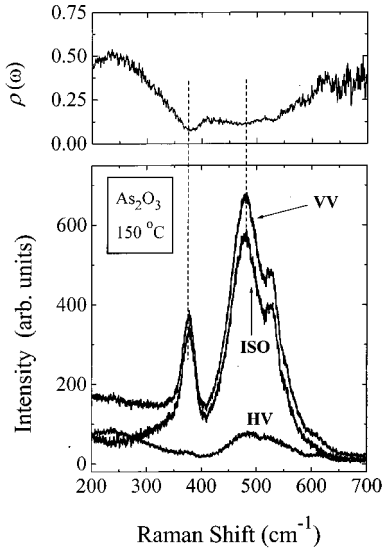

FIG. 2. Polarized (VV), depolarized (HV), and isotropic (ISO) Raman spectra for As_2O_3 at 150 °C, ($T_g \approx 160$ °C). Dashed lines mark the positions of the individual vibrational lines that have been analyzed in the present work. The respective depolarization ratio $\rho(\omega)$ is plotted in the upper part of the figure.

tra, $\rho(\omega)$, in order to locate the vibrational lines in the full energy range recorded. The analysis showed that the Raman spectra of As_2O_3 (Fig. 2) consist of the depolarized weak, broad line at $\omega \approx 240$ cm^{-1}, the totally polarized sharp peak at $\omega \approx 378$ cm^{-1}, and the group of strongly polarized lines at $\omega \approx 480$, 530, and in the range 550–600 cm^{-1}. For the $2BiCl_3$–KCl system (Fig. 3) there is a totally depolarized weak, broad line at $\omega \approx 145$ cm^{-1}; the line at $\omega \approx 265$ cm^{-1} ($\rho \approx 0.25$) and the more intense, strongly polarized line ($\rho \approx 0.10$) located at $\omega \approx 308$ cm^{-1} form an overlapped doublet. Assignment of the vibrational modes for As_2O_3 and $2BiCl_3$–KCl can be found in Refs. 13(b) and 22, respectively.

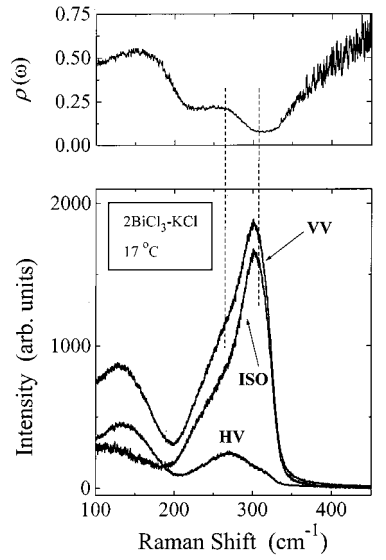

FIG. 3. Polarized (VV), depolarized (HV), and isotropic (ISO) Raman spectra for $2BiCl_3$–KCl at 20 °C ($T_g \approx 37$ °C). Dashed lines mark the positions of the individual vibrational lines that have been analyzed in the present work. The respective depolarization ratio $\rho(\omega)$ is plotted in the upper part of the figure.

The usual approach to obtain information about the molecular dynamics from the Raman spectra is to numerically Fourier transform the spectra so as to obtain TCF and to fit the obtained TCF with a particular model. To follow this procedure one first has to locate an isolated (nonoverlapping) line in the spectrum, a fact that can hardly be realized in a wide gamut of inorganic materials. This means that overlapping lines, as in the present work, could not be used unambiguously for studying molecular dynamics.

This problem can be avoided by employing a TCF that has an analytical counterpart in the frequency domain. In this case one can obtain correlation times for single or composite lines through fits in the frequency domain without using Fourier transforms.[23] The method is based on the TCF of the following form:[24]

$$G_V(t) = \exp\{-[(t^2+\tau_1^2)^{1/2}\tau_1]/\tau_2\}. \tag{10}$$

The FT of Eq. (10) is analytical, leading to the following expression for the vibrational line profile:

$$I(\nu) = 2c \exp(\tau_1/\tau_2)(\tau_1^2/\tau_2)K_1(x)/x, \tag{11}$$

where

$$x = \tau_1[4\pi^2c^2(\nu-\nu_0)^2 + 1/\tau_2^2]^{1/2}, \tag{12}$$

where $\mathbf{K}_1(x)$ is the modified Bessel function of the second kind, $\nu = \omega/2\pi c$ is the wave number, ν_0 is the peak position. It has been shown[23] that the TCF defined in Eq. (10) covers the whole domain of definition of Eq. (7), with τ_1 being close to τ_ω, and τ_2 to τ_V. Application of Eqs. (1) and (11) to the studies of dynamics in various liquid and glassy systems can be found elsewhere.[21(c),25]

It should be mentioned here that Eqs. (10) and (11) are applicable not only in the case of Gaussian–Markovian modulation. They can also account for vibrational dephasing processes caused by non-Markovian[26] and purely discrete Markovian modulation,[27] which lead to quite noticeable deviations of the line profile from Gaussian-type or Lorentzian-type forms.

The computation procedure based on Eqs. (10) and (11) is as follows: The composite spectrum is fitted to Eq. (11) in order to find the τ_1 and τ_2 times for each vibrational line. After having found these values, each line can be recovered and its second moment M_2, can be determined. Then, the corresponding TCFs, Eq. (10), are calculated; the τ_V values are found as the integrals over respective TCFs, and finally Eq. (7) is fitted to TCFs in order to obtain the values of τ_ω.

In the case of arsenic oxide the fits were made in the region 200–700 cm^{-1} due to the absence of peaks in the isotropic Raman spectra below 200 cm^{-1}. During the fitting procedure we have taken into account the isotropic lines located at 378, 480, 530, and 550 cm^{-1}, as well as a broad band at 360 cm^{-1}. Representative fits of the Raman spectra of arsenic oxide are given in Fig. 4. As can be seen from the residual plot (at the bottom of the figure), the difference between experimental and fitting data does not exceed background noise values. The quality of the fits of the strongest

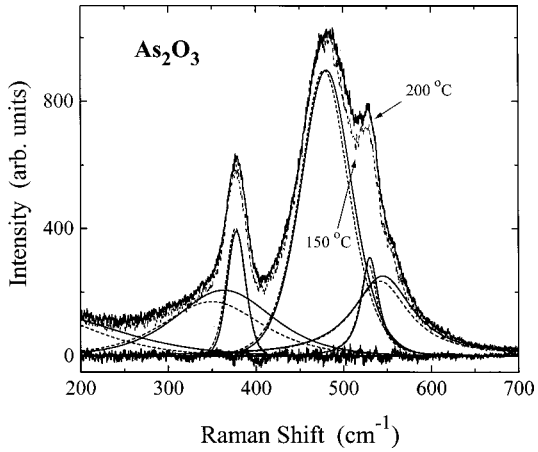

FIG. 4. Isotropic spectra for As_2O_3 and individual fitted curves at two temperatures close to the glass transition temperature. Solid lines correspond to 200 °C and dashed lines to 150 °C.

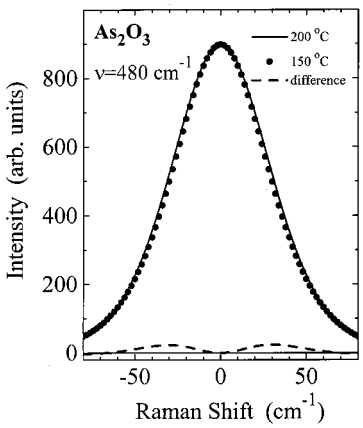

FIG. 6. Isotropic line profiles of the 480 cm^{-1} vibrational mode for As_2O_3 at 200 °C (solid line) and 150 °C (solid circles). The two data sets have been normalized to the same maximum intensity in order to compare the line profiles. The dashed line at the bottom of the curve shows the difference between the two line profiles.

lines at 378 and 480 cm^{-1} is considered quite satisfactory. Some distortions take place at the overlap of the high-frequency wing of the former line and the low-frequency wing of the latter, but they are still within the limits of the background noise. The same is true for the less-intensive lines located at 530 and 550 cm^{-1} as well. The quality of fitting of the broad band at 360 cm^{-1} is not so high compared to other lines.

The results reveal that either in the melt (above T_m), in the supercooled phase, or in the glass the line profiles are always close to Gaussian, since the inequality $\tau_1 \geqslant \tau_2$ is indicative for the Gaussian profiles. This finding implies that in all phases the environment around the probe vibrator should be considered frozen (slow modulation limit). The characteristic times, τ_1 and τ_2, analogues of the modulation and vibrational relaxation characteristic times, are presented in Fig. 5. The temperature dependence of τ_2 for both vibrational modes is continuous, experiencing no significant changes at T_m and T_g, which are indicated by dashed lines. On the other hand, the temperature dependence of the relaxation time τ_1 exhibits an unexpected *jump discontinuity* near T_g. Qualitatively similar results have been obtained for the vibrational lines located at 530 and 550 cm^{-1}. Since these last two lines are weak and therefore the associated error bars significant, we have chosen to deal with only the 378 and 480 cm^{-1} lines.

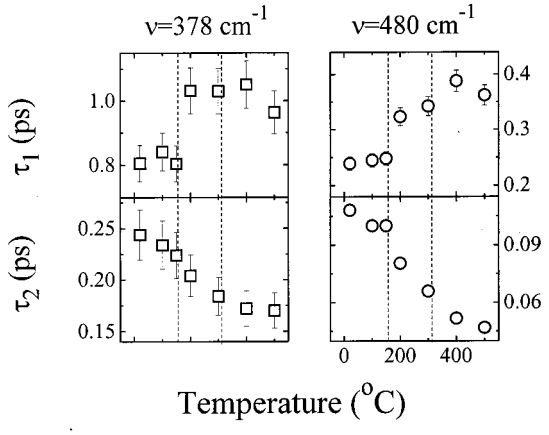

FIG. 5. Temperature dependence for the characteristic times τ_1 and τ_2 for As_2O_3 as extracted from the fitting of the experimental isotropic spectra with Eq. (11). The glass transition temperature and the melting point are shown as dashed vertical lines. τ_1 and τ_2 are used to calculate the relaxation times τ_ω and τ_V, respectively, as described in the text.

Another important finding emerging from Fig. 5 is that the time τ_1 becomes shorter as the temperature is lowered below T_g or, in terms of TCFs, the modulation process becomes faster in the glass than in liquid. Regarding line profiles, this means that the lines in the glass become ''less'' Gaussian in shape than in the melt and the supercooled state.

In order to analyze these results in more detail, we compare the line profiles obtained at temperatures close to T_g, where the corresponding changes in τ_1 are substantial. The line profiles are normalized to the peak maximum intensity of the lower temperature spectrum. As becomes evident from Fig. 4, the changes in all line profiles are notable, indicating possible changes in vibrational dynamics. To better discern the modifications of the line shapes we present Fig. 6, where the environment-induced variations occurring in the profile of the 480 cm^{-1} vibrational lines are shown. It is obvious that the line profile is changing below T_g. The difference in the distribution of intensities shown by the dashed line in Fig. 6 significantly exceeds the background noise. Comparison between the profiles of other lines reveals similar behavior.

The characteristic times τ_1 and τ_2, extracted from the fitting analysis, were used as inputs to calculate TCFs through Eq. (10) and to find relevant dynamics parameters (M_2, τ_ω, and τ_V). Representative TCFs are given in Fig. 7; they perfectly follow the Kubo law and reveal an increasing dephasing rate upon heating. The temperature dependence of dynamic parameters along with linewidths and peak frequencies are shown in Fig. 8.

In the case of the $2BiCl_3$–KCl glass-forming mixture, the overlap of the low-frequency features with the vibrational lines is more significant, necessitating the employment of a composite fit including the whole spectral region, i.e.,

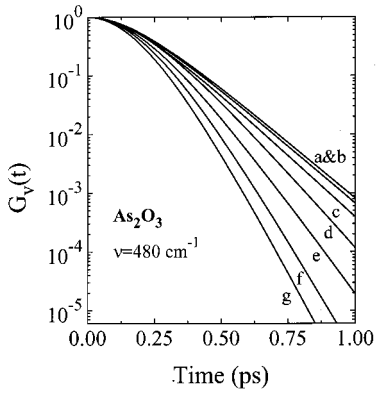

FIG. 7. Semilogarithmic plots of time-correlation functions corresponding to the line profiles of the 480 cm^{-1} vibrational mode for As_2O_3 at different temperatures: (a) 20 °C; (b) 100 °C; (c) 150 °C; (d) 200 °C; (e) 300 °C; (f) 400 °C; (g) 500 °C.

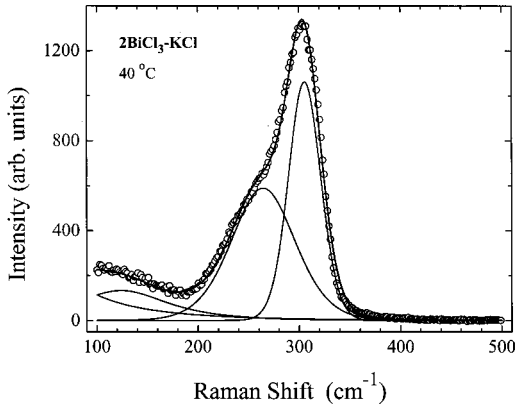

FIG. 9. Representative fit for the 40 °C isotropic spectrum of $2BiCl_3$–KCl. Open circles denote the experimental data, while the solid lines correspond to the individual vibrational modes. The thick solid line represents the total fitted curve. Only one-tenth of the experimental points is shown for clarity.

15–500 cm^{-1}. As follows from Fig. 9, the difference between experimental and calculated values is of the order of magnitude of the background noise in the low-frequency region, but the quality of fits is lower for the high-frequency modes. The residuals do not exceed 5% of the total intensity of the raw data, but they overwhelm the background noise level more than 3 times. Therefore, the dynamic parameters obtained for the $2BiCl_3$–KCl glass-forming mixture are less precise than those for arsenic oxide. Undoubtedly, the fit could be improved by taking into account an extra peak at this region, but we prefer to keep the parametrization of the problem to the lowest possible extent.

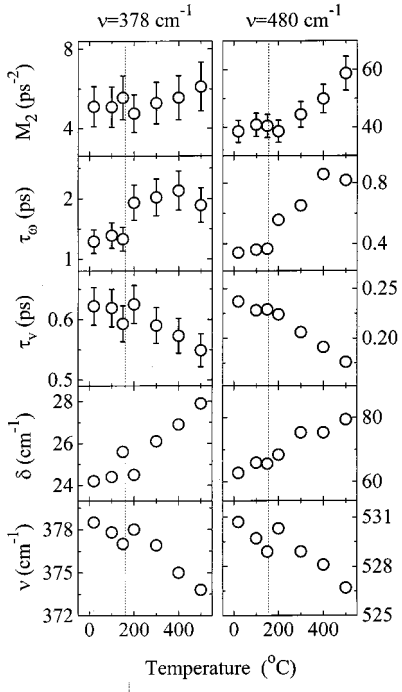

FIG. 8. Temperature dependence for various parameters of the 378 cm^{-1} (left part) and 480 cm^{-1} (right part) vibrational modes of As_2O_3. ν: peak position; δ: half-width; τ_V: vibrational relaxation time; τ_ω: modulation time; M_2: second moment. The error bars are less than the symbol size in the case where they are not shown.

Following the aforementioned procedure for As_2O_3, these results suggest that the line profiles of the $2BiCl_3$–KCl mixture are close to Gaussian, and therefore in all phases the environment of probe particles can also be considered frozen. The temperature dependence of τ_V undergoes a break, while that of τ_ω exhibits a *jump discontinuity* at temperatures close to T_g; see Fig. 10. We observe once again that τ_ω becomes shorter below T_g, i.e., the modulation process becomes faster in the glass than in the liquid, and the lines in the glass become ''less Gaussian'' in shape than in the normal and supercooled liquid. Comparing the line profiles obtained at temperatures around the glass transition region, where the changes in τ_ω were more pronounced, we reassure that these profiles do indeed change below T_g. As in the case of arsenic oxide, the difference in the distribution of intensities is significantly exceeding the background noise; Fig. 11. Representative TCFs for $2BiCl_3$–KCl are presented in Fig. 12.

B. Vibrational dephasing and vibrational frequency modulation at temperatures around T_g: Discussion in the framework of existing theories

As results from the preceding section show, the line profiles for the two glass-formers of different fragility, chemical nature, and molecular structure studied in this work exhibit similar behavior at all temperatures, in all phases. This result seems rather unexpected at a first glance. Before discussing the spectral features of the line profiles, we will first recall some important issues pertaining to the structure of the materials studied.

It is a well-established fact[12(b)] that in systems where strong intermolecular interactions or steric hindrances prevail (glasses, polymers, liquid crystals, etc.), vibrational lines have Gaussian profiles (Gaussian–Markovian modulation, Kubo case[15,16]) or even over-Gaussian (hierarchically constrained modulation[26]). As_2O_3 is a network-like glass formed by ''infinite'' two-dimensional layers with strong covalent intralayer bonding and weak short-range van der Waals interlayer interactions. From this point of view, it is reasonable to anticipate Gaussian profiles of vibrational lines in As_2O_3.

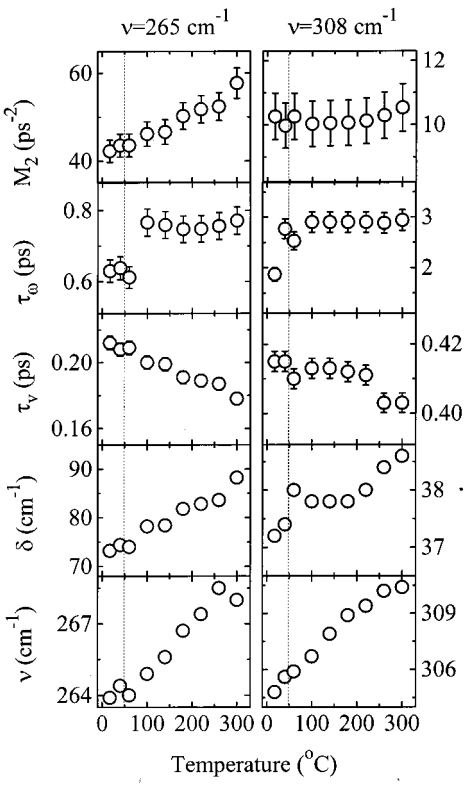

FIG. 10. Temperature dependence for various parameters of the 265 cm^{-1} (left part) and 308 cm^{-1} (right part) vibrational modes of $2BiCl_3$–KCl. ν: peak position; δ: half-width; τ_V: vibrational relaxation time; τ_ω: modulation time; M_2: second moment. The error bars are less than the symbol size in the case where they are not shown.

On the other hand, the $2BiCl_3$–KCl mixture is an ionic liquid where strong, long-range forces dominate. Some predictions suggesting that long-range forces are responsible for inhomogeneous broadening and Gaussian line shapes[17(b)] are not valid for molten salts. Long-range Coulombic forces do not contribute to the spectroscopically active part of the interparticle potential, and therefore are ''invisible'' in vibrational spectroscopy.[12(b),28] A long body of experimental data shows that the line broadening in simple molten salts with complex anions is mainly homogeneous. This implies that modulation events are caused by collisions, repulsion forces prevail, and the respective line profiles are close to Lorentzian ones.[12(b)] When ion-induced dipole forces play the major role in collision processes, as in similar halide systems ($MnCl_2$–CsCl and $ZnCl_2$–CsCl),[25(b)] line profiles become over-Lorentzian in shape, and modulation events are a purely discrete Markovian process.[27]

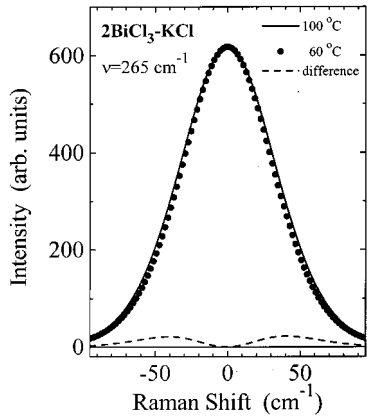

FIG. 11. Isotropic line profiles of the 265 cm^{-1} vibrational mode for $2BiCl_3$–KCl at 100 °C (solid line) and 60 °C (solid circles). The two data sets have been normalized to the same maximum intensity in order to compare the line profiles. The dashed line at the bottom of the curve shows the difference between the two line profiles.

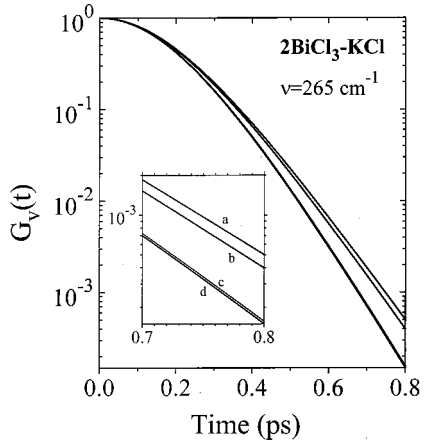

FIG. 12. Semilogarithmic plots of time-correlation functions corresponding to the line profiles of the 265 cm^{-1} vibrational mode for $2BiCl_3$–KCl at different temperatures: (a) 17 °C; (b) 40 °C; (c) 100 °C; (d) 140 °C. The inset shows an enlargement of the slow time limit.

Similar vibrational line broadening caused by the slow Gaussian–Markovian modulation events in two glass formers of distinctly different nature suggests that strong intermolecular interactions or steric hindrances play the major role in picosecond dynamics of these systems and lead to the ''freezing'' of the environment of the probe vibrators on time scales slower than those characterizing the vibrational energy relaxation. In other words, collisions, or more generally interactions, which give rise to phase shifts, are quite slow. For the strong As_2O_3 this is expected due to its network-like structure that persists even at high temperatures, preventing fast diffusional motions. On the other hand, for the fragile $2BiCl_3$–KCl it seems that the highest temperature employed in this work is not sufficient to enhance diffusivity so as to allow subpicosecond motions

To analyze the temperature dependence of dephasing times in the Gaussian–Markovian (Kubo) case, one can apply numerous theories[17] where τ_V^{-1} has been predicted to depend on density, viscosity, and temperature. Since all these properties are continuous functions of the temperature, we expect that the temperature dependence of linewidths is also continuous around T_g.

The temperature dependence of vibrational frequency modulation time τ_ω for both substances under study exhibits a *jump discontinuity* in the neighborhood of the glass transition temperature. The only quantity which behaves similarly when traversing the glass transition region is the heat capacity;[29] other second derivatives of thermodynamic and kinetic parameters of glass-forming systems are continuous functions of temperature at T_g. Furthermore, it appears that

in the glass the modulation times become shorter, i.e., the modulation process becomes faster than in the liquid state. This means that the line profile in the glass becomes ''less Gaussian,'' and the environment of the probe vibrator appears ''less static'' than in the liquid. None of the existing theories predicts specific changes in τ_ω for ''more'' static or ''less'' static cases.[11,12,15]

Frequently, modulation processes in theories treating dephasing in the Kubo spirit are described in terms of the Enskog (isolated binary collision) model.[30] This model determines the time between collisions τ_{BC}, which is considered equal to τ_ω, as

$$\tau_{\mathrm{BC}}=\frac{1}{4\sigma^2 N g(\sigma)}\sqrt{\frac{2\mu}{\pi k_B T}}=\frac{V_M}{4\sigma^2 N_A g(\sigma)}\sqrt{\frac{2\mu}{\pi k_B T}}, \tag{13}$$

where σ is the collision diameter, $N=N_A/V_M$ is the number density, N_A is the Avogadro number, V_M is the molar volume, $g(\sigma)$ is the radial distribution function which may be considered equal to unity,[30] μ is the reduced mass of colliding particles, k_B is the Boltzmann's constant, and T is the temperature.

Using the isolated binary collision model, one may face several complications caused by its qualitative nature.[30] On the other hand, the final equations of an alternative theory[31] and most recent improvements of the Enskog model[32] have been formulated in a nonanalytical form and cannot be directly employed in dephasing theories. Further, in the slow modulation limit, the size and mass of big molecular aggregates becomes indefinite. Therefore, the use of the Enskog equation can be justified for, at least, rough estimates of the nature of modulation events.

The temperature dependence of τ_{BC} is determined by the ratio $V_M/\sqrt{T}$ in Eq. (13). This means that upon heating, the time between collision has to increase as a result of the thermal expansion (V_M in the numerator) while it has to decrease as a result of thermal agitation of molecular motion (T in the denominator). Either in molten salts or in aqueous solutions,[12(b)] modulation times are not sensitive to the variations of temperature. In organic liquids, modulation times often increase on heating, thus exhibiting the prevalence of thermal expansion effects. It is obvious from the above discussion that Eq. (13) is able to predict any *smooth* temperature dependence of the modulation time, since the molar volume always changes smoothly if a second-order phase transition is not present. However, Eq. (13) fails in describing the observed discontinuity in the temperature dependence of the modulation time near T_g.

C. Possible implications of cooperative dynamics in the vibrational dynamic anomaly

The idea behind the pursuit of a possible connection between vibrational dynamics and cooperativity stems from the fact that vibrational dynamics is extremely sensitive to intermolecular or ''environmental'' interactions. The latter (intermolecular interactions) are ultimately responsible for the sluggish dynamics, which ahs been named cooperativity, approaching T_g. Then, it is plausible to consider that vibrational dynamics and cooperative dynamics sharing the common influence of intermolecular interactions should also be related.

In a very general definition, the vibrational relaxation rate is related to the Enskog rate through[33]

$$t_V^{-1}=\kappa\tau_{\mathrm{BC}}^{-1}, \tag{14}$$

where κ is a probability factor determining the ability of modulation attempts to produce dephasing. Among other parameters controlling the dephasing rate this probability factor, κ, incorporates steric or geometrical factors. Steric factors have already been explicitly employed in some dephasing theories.[17(b)] Since ''collisions'' or, more generally interactions are the motive force for vibrational dephasing and modulation events, then steric factors play the role of an effective cross section enabling to discern between ''successful'' interactions, which cause phase shifts, and ''unsuccessful'' ones. In close resemblance with chemical kinetics, we might envisage the aforementioned probability factor as a kind of a ''transmission factor.''[34] Furthermore, introducing such a factor, one can smoothly pass from the fast to the slow modulation limit for the same species even at small variations of collision rates.

The transmission factor could be somehow related to cooperative effects in glass-forming liquids, especially in those governed by restrictions in molecular movements that involve orientational and/or translational motion. In particular, in the framework of the lattice–gas models[7(a)] cooperativity has been claimed to appear as a result of certain geometrical restrictions in the hopping pathways. Specifically, even in the two-dimensional triangular lattice, cooperative effects arise if—in addition to the requisite of an empty destination site for the hopping particle—the neighboring sites to the hopping path are also empty. Such restrictions can be incorporated in a generalized transmission factor. An immediate consequence of the aforementioned restrictions in hopping pathways is the occurrence of permanently immobile particles in lattices, forming rings (convex polygons). Further support for the existence of long-lived structures in a fragile glass-forming Lennard-Jones mixture has been found in molecular dynamics simulations conducted in three-dimensional space.[8(b)] These data showed that stringlike structures might persist in such systems even at temperatures well above T_g, with the string length growing upon cooling.

Finally, either lattice–gas models or molecular simulations in Lennard–Jones systems have been dealing with spherical, structureless particles. In our case, the structural units that constitute the glasses studied are certain coordination polyhedra. It would thus be instructive to make a step forward assuming that in the glassy state such structural units, being arranged in rings, layers, etc., might retain at least some specific orientational order. Such ordering, while approaching the glass transition temperature, is expected to facilitate the vibrational phase shifts and, in fact, to enhance the magnitude of the transmission factor for these processes. To better understand the relation between vibrational features and structural reorganization that eventually leads to cooperativity, one may recall here that intermolecular interactions depend upon two important factors: first, on the intermolecu-

lar distances and second, on the mutual orientations of at least the molecules that form the first coordination shell around the probe molecule. Intermolecular distances have trivial temperature dependence and are not expected to be the key factor leading to the observed anomaly of the temperature dependence of τ_ω. On the other side, molecular organization—resulting from the requirement of a specific disposition of molecules around the probe ''particle'' in the energetically favored orientations—is the cause of the formation of complex structural arrangements (rings, strings, polygons, etc.). The latter, on the one hand, enhance the possibility or the effectiveness of dephasing due to the strengthening of interactions (jump discontinuity in the temperature dependence of modulation times τ_ω), and on the other hand engender cooperativity due to the involvement of many-molecule clusters. On the contrary, in the moderately supercooled and in the normal liquid state the transmission factor (or the effectiveness of interactions) is expected to decrease due to the enhancement of the orientational disorder; thus, not all interactions are successful and the rate of phase shifts becomes slower. Finally, considering that intermolecular potentials consist of a radial and an angular (orientational) part, the experimental findings of the present paper and the above discussion suggest that the orientational part is the one that predominates while approaching T_g, and it seems to be responsible for the ''switching on'' of the anisotropic interactions which causes the anomalous temperatures dependence of τ_ω.

Before closing this section it would be instructive to mention that a jump discontinuity in the temperature dependence of *vibrational relaxation* times has been observed in the phase transition ice→water.[35] In that work the vibrational lifetime of the OH-stretching mode was directly measured using time-domain techniques. Apart from the discontinuity, the vibrational lifetime was found to increase monotonically when temperature increases. To account for this last finding, the authors invoked the temperature dependence of two parameters, namely the density and the average hydrogen-bond strength, concluding that the latter plays the dominant role. This shows that thermodynamic quantities (like density) are not able to account for the monotonic smooth increase of the vibrational lifetime with temperature, and therefore they are even less suitable for explaining jump discontinuities like the ones observed in our experiments. Finally, in analogy with the results described above, i.e., a jump discontinuity when crossing a phase transition, we could envisage the onset of some ''transition'' when approaching T_g. This particular transition might be associated with the switching on of stronger interactions between molecular units due to the formation of bound aggregate states, leading finally to the enhancement of the effectiveness of the modulation events.

V. CONCLUDING REMARKS

In this paper we have made an attempt to analyze the changes that certain parameters, related to vibrational relaxation and vibrational frequency modulation, experience as a result of supercooling particular glass-forming liquids. Raman spectra for a fragile and a strong glass-former have been measured in the liquid, supercooled, and glassy state. Selected bands have been analyzed in the framework of vibrational relaxation theories.

We have shown that the vibrational line profiles follow the Kubo–Rothschild line-shape model. The temperature dependence of linewidths for both glasses undergoes a break (change in the slope) at temperatures close to T_g. The vibrational lifetime decreases monotonically with temperature, as is predicted in most theories. All line profiles are close to the Gaussian form, revealing that in all phases, i.e., melt, supercooled liquid, and glass, the environment around the probe vibrator is considered as being frozen (slow modulation limit). An unexpected finding is that the frequency modulation times become shorter below T_g and hence modulation processes become faster in the glass than in the liquid.

In an attempt to account for these findings, we have resorted to a parameter incorporating steric or geometrical effects. For this reason, the idea of a transmission or probability factor enabling to discern between ''successful'' collisions causing phase shifts and ''unsuccessful'' ones, has been adopted. Referring to the existing models and simulations of glass-forming systems, it seems that ordering effects (arrangements in rings, convex polygons, or strings) in these systems are considered to arise from some geometrical restrictions bearing a close resemblance to the transmission factor.

It should be stressed that in studies concerning cooperativity in glass-forming systems one has to discern between parameters which sense cooperativity in different ways. There are *dynamical* variables that do reflect cooperativity rather directly, which exhibit pronounced changes at the vicinity of T_g, i.e., the viscosity or the α-relaxation time. On the other hand, there are *thermodynamic* quantities like the density, the coefficient of thermal expansion, and the compressibility, whose magnitude is also determined by the intermolecular forces, but do not experience in a direct way the presence of cooperative dynamics. The temperature dependence of such thermodynamic quantities is quite normal in the sense that it does not exhibit singularities or jumps near T_g; only subtle slope changes are observed in experimental data.

The cooperativity-sensitive indicator we have used in the present work is the temperature dependence of a *dynamical* variable, namely the modulation time τ_ω. We have argued that this variable might be a suitable indicator of cooperativity since it depends upon the intermolecular interactions which ultimately are responsible for the cooperative or sluggish dynamics when approaching T_g. Further, its temperature dependence at the vicinity of T_g may be satisfactorily rationalized, at least on a qualitative basis, in terms of transmission factors. Finally, it has been stressed recently that the description of dynamics based on ensemble averaged quantities needs to be modified in order to apply to supercooled materials, and spatial averages for the glassy state should be replaced by local response functions.[36] One may assume that operating with more correct models will significantly improve the description of the temperature dependence of modulation times and even explain its discontinuity at T_g.

Concluding, we would like to emphasize that for a

deeper comprehension of the role played by cooperativity in vibrational dynamics in supercooled liquids and glasses, more systematic treatment has to be undertaken. In particular, studies of vibrational dynamics of viscous liquids confined in restricted geometries, could be quite informative. Preliminary data for glass-forming substances in our group show that vibrational dynamics becomes faster under confinement. The similar behavior exhibited by the α-relaxation process (i.e., facilitation of structural relaxation) due to removal of cooperativity under confinement[37] seems to be compelling evidence that vibrational dynamics does indeed sense cooperativity.

ACKNOWLEDGMENTS

This work was supported in terms of the NATO collaborative linkage grant (CLG.977358) and the Greek–Ukrainian bilateral collaboration (ETTAN-M.4.3:2013555).

[1] See, for example, *Proceedings of the Third International Discussion Meeting on Relaxations in Complex Systems*, edited by K. L. Ngai, E. Riande, and M. D. Ingram [J. Non-Cryst. Solids **235–237** (1998)], entire issue.
[2] K. L. Ngai and R. W. Rendell, in *Supercooled Liquids: Advances and Novel Applications*, edited by J. Fourkas, D. Kivelson, U. Mohanty, and K. Nelson, ACS Symposium 676 (American Chemical Society, Washington, DC, 1997), pp. 45–66.
[3] G. Adam and J. H. Gibbs, J. Chem. Phys. **43**, 139 (1965).
[4] (a) W. G. Rothschild, *Dynamics of Molecular Liquids* (Wiley, New York, 1984); (b) C. H. Wang, *Spectroscopy of Condensed Media. Dynamics of Molecular Interactions* (Academic, Orlando, 1985).
[5] E. Donth, J. Non-Cryst. Solids **53**, 325 (1982); E. Donth, *Relaxation and Thermodynamics in Polymers: Glass Transition* (Akademie, Berlin, 1992).
[6] K. L. Ngai, J. Chem. Phys. **111**, 3639 (1999).
[7] (a) J. Jäckle and A. Kronig, J. Phys.: Condens. Matter **6**, 7633 (1994); (b) S. Eisinger and J. Jäckle, J. Stat. Phys. **73**, 643 (1993).
[8] (a) R. D. Mountain, J. Chem. Phys. **102**, 5408 (1995); (b) C. Donati, J. F. Douglas, W. Kob, S. J. Plimpton, P. H. Poole, and S. C. Glotzer, Phys. Rev. Lett. **80**, 2338 (1998); for a recent review see S. C. Glotzer, J. Non-Cryst. Solids **274**, 342 (2000).
[9] (a) R. Richert, Phys. Rev. B **54**, 15762 (1996); (b) M. Arndt, R. Stannarius, H. Groothues, E. Hempel, and F. Kremer, Phys. Rev. Lett. **79**, 2077 (1997); (c) M. T. Cicerone, F. R. Blackburn, and M. D. Ediger, J. Chem. Phys. **102**, 471 (1995); (d) A. K. Rizos and K. L. Ngai, Phys. Rev. E **59**, 612 (1999); (e) U. Tracht, M. Wilhelm, A. Heuer, H. Feng, K. Schmidt-Rohr, and H. W. Spiess, Phys. Rev. Lett. **81**, 2727 (1998).
[10] E. Vidal Russell and N. E. Israeloff, Nature (London) **408**, 695 (2000).
[11] D. W. Oxtoby, Adv. Chem. Phys. **40**, 1 (1979); **47**, 487 (1981); Annu. Rev. Phys. Chem. **32**, 77 (1981).
[12] (a) O. F. Nielsen, Annu. Rep. Prog. Chem., Sect. C: Phys. Chem. **90**, 3 (1993); **93**, 57 (1997); (b) S. A. Kirillov, J. Mol. Liq. **76**, 35 (1998).
[13] (a) V. G. Akhtyrsky, S. A. Kirillov, and V. D. Prisyazhnyi, Fiz. Khim. Stekla **5**, 56 (1979); (b) G. N. Papatheodorou and S. A. Solin, Phys. Rev. B **13**, 1741 (1976); (c) H. G. K. Sundar, R. Parthasaraty, and K. J. Rao, Z. Naturforsch. A **37a**, 191 (1982); S. Ganguly, R. Parthasaraty, K. J. Rao, and C. N. Ramachandra Rao, J. Chem. Soc., Faraday Trans. 2 **80**, 1395 (1984).
[14] (a) K. D. Rector and M. D. Fayer, J. Chem. Phys. **108**, 1794 (1998); (b) K. D. Rector, A. S. Kwok, C. Ferrante, R. S. Francis, and M. D. Fayer, Chem. Phys. Lett. **276**, 217 (1997); (c) M. D. Fayer and D. T. Dlott, in *Supercooled Liquids: Advances and Novel Applications*, edited by J. Fourkas, D. Kivelson, U. Mohanty, and K. Nelson, ACS Symposium 676 (American Chemical Society, Washington, DC, 1997), pp. 324–337.
[15] (a) R. G. Gordon, J. Chem. Phys. **43**, 1307 (1965); (b) R. Kubo, in *Fluctuations, Relaxation, and Resonance in Magnetic Systems*, edited by G. ter Haar (Plenum, New York, 1962), p. 27.
[16] (a) M. Constant and R. Fauquembergue, J. Chem. Phys. **58**, 4030 (1973); (b) W. G. Rothschild, *ibid.* **65**, 455 (1976).
[17] (a) R. M. Lynden-Bell, Mol. Phys. **33**, 907 (1977); S. C. Fischer and A. Laubereau, Chem. Phys. Lett. **51**, 189 (1978); D. W. Oxtoby, J. Chem. Phys. **70**, 2605 (1979); (b) K. S. Schweizer and D. Chandler, *ibid.* **76**, 2296 (1982).
[18] R. Zwanzig, J. Chem. Phys. **34**, 1931 (1961).
[19] S. A. Egorov and J. L. Skinner, J. Chem. Phys. **103**, 1533 (1995); **105**, 10153 (1996); **112**, 275 (2000); S. A. Egorov, K. F. Everitt, and J. L. Skinner, J. Phys. Chem. A **103**, 9494 (1999); R. E. Larsen and R. M. Stratt, J. Chem. Phys. **110**, 1036 (1999); G. Gershinsky and B. J. Berne, *ibid.* **110**, 1053 (1999).
[20] R. E. Wilde, Mol. Phys. **57**, 675 (1986); R. E. Wilde and J. Yarwood, J. Raman Spectrosc. **19**, 289 (1988).
[21] (a) S. N. Yannopoulos, G. N. Papatheodorou, and G. Fytas, Phys. Rev. B **60**, 15131 (1999); (b) S. N. Yannopoulos, G. N. Papatheodorou, and G. Fytas, J. Chem. Phys. **107**, 1341 (1997); (c) S. A. Kirillov and S. N. Yannopoulos, Phys. Rev. B **61**, 11391 (2000).
[22] K. W. Fung, G. M. Begun, and G. Mamantov, Inorg. Chem. **12**, 53 (1973).
[23] S. A. Kirillov, Chem. Phys. Lett. **303**, 37 (1999).
[24] P. A. Egelstaff and P. Schofield, Nucl. Sci. Eng. **12**, 260 (1962).
[25] (a) S. A. Kirillov and O. Faurskov Nielsen, J. Mol. Struct. **526**, 317 (2000); (b) S. A. Kirillov, G. A. Voyiatzis, I. N. Musiyenko, G. M. Photiadis, and E. A. Pavlatou, J. Chem. Phys. **114**, 3683 (2001).
[26] W. G. Rothschild, M. Perrot, and F. Guillaume, Chem. Phys. Lett. **128**, 591 (1986); J. Chem. Phys. **87**, 7293 (1987); S. A. Kirillov, Chem. Phys. Lett. **200**, 205 (1992).
[27] S. G. Fedorenko, A. Yu. Pusep, and A. I. Burshtein, Spectrochim. Acta, Part A **43A**, 483 (1987); S. A. Kirillov and T. M. Kolomietz, *ibid.* **48A**, 867 (1992); S. A. Kirillov, Chem. Phys. Lett. **202**, 459 (1993).
[28] S. A. Kirillov and A. V. Gorogyskii, Dokl. Akad. Nauk SSSR **261**, 1371 (1981).
[29] R. Zallen, *Physics of Amorphous Solids* (Wiley, New York, 1983).
[30] P. S. Dardi and R. I. Cukier, J. Chem. Phys. **89**, 4145 (1988); **95**, 98 (1991).
[31] S. A. Adelman and R. H. Stote, J. Chem. Phys. **88**, 4397 (1988); R. H. Stote and S. A. Adelman, *ibid.* **88**, 4415 (1988); S. A. Adelman, R. Muralidhar, and R. H. Stote, *ibid.* **95**, 2738 (1991).
[32] K. Miyazaki, G. Srinivas, and B. Bagchi, J. Chem. Phys. **114**, 6276 (2001); B. Bagchi, G. Srinivas, and K. Miyazaki, *ibid.* **115**, 4195 (2001).
[33] K. F. Herzfeld and T. A. Litovitz, *Absorption and Dispersion of Ultrasonic Waves* (Academic, New York, 1959).
[34] To better understand the role of the transmission factor, recall that in chemical kinetics, many reactions are favored for certain relative orientations of particles. In such cases, it is usually assumed that the "reactivity" of the probe particle is not uniform over its surface. It depends on the polar angle θ measured from an axis fixed on the molecule and pointing through the region of maximum "reactivity." This means that the rate of reaction k cannot be expressed only in terms of average thermal velocities u_0, $k \propto u_0$, and becomes dependent on the orientation of reactants, $k \propto u_0 f(\theta)$, $f(\theta) < 1$, where $f(\theta)$ is considered as the transmission factor. This formalism is equally applicable to any kind of reactions, including vibrational deactivation.
[35] S. Woutersen, U. Emmerichs, H.-K. Nienhuys, and H. J. Bakker, Phys. Rev. Lett. **81**, 1106 (1998).
[36] R. Richert, J. Chem. Phys. **114**, 7471 (2001).
[37] K. L. Ngai, J. Phys.: Condens. Matter **11**, A119 (1999).